Generation of ultrashort electron bunches by colliding laser pulses

C. B. Schroeder, P. B. Lee, and J. S. Wurtele
Department of Physics, University of California at Berkeley, Berkeley, California 94720

E. Esarey and W. P. Leemans
Center for Beam Physics, Ernest Orlando Lawrence Berkeley National Laboratory, Berkeley, California 94720

(Received 17 August 1998; revised manuscript received 14 January 1999)

A proposed laser-plasma-based relativistic electron source [E. Esarey *et al.*, Phys. Rev. Lett. **79**, 2682 (1997)] using laser-triggered injection of electrons is investigated. The source generates ultrashort electron bunches by dephasing and trapping background plasma electrons undergoing fluid oscillations in an excited plasma wake. The plasma electrons are dephased by colliding two counterpropagating laser pulses which generate a slow phase velocity beat wave. Laser pulse intensity thresholds for trapping and the optimal wake phase for injection are calculated. Numerical simulations of test particles, with prescribed plasma and laser fields, are used to verify analytic predictions and to study the longitudinal and transverse dynamics of the trapped plasma electrons. Simulations indicate that the colliding laser pulse injection scheme has the capability to produce relativistic femtosecond electron bunches with fractional energy spread of order a few percent and normalized transverse emittance less than 1 mm mrad using 1 TW injection laser pulses.
[S1063-651X(99)04505-5]

PACS number(s): 52.40.Nk, 41.75.Lx, 29.25.Bx

I. INTRODUCTION

Plasma-based accelerators [1–3] have received much theoretical and experimental attention owing to the extremely high longitudinal electric fields that can be excited in a plasma without the limitations due to breakdown found in conventional accelerators. The characteristic scale length of the accelerating field (plasma wake) in a plasma-based accelerator is the plasma wavelength $\lambda_p\ (\mathrm{m}) = 2\pi c/\omega_p \simeq 3.3 \times 10^4 n_e^{-1/2}\ (\mathrm{cm}^{-3})$, where n_e is the plasma density, c is the speed of light, and $\omega_p = (4\pi n_e e^2/m_e)^{1/2}$ is the plasma frequency with m_e the electron mass and $-e$ the electron charge. In such short wavelength accelerators (typically $\lambda_p \lesssim 100\ \mu\mathrm{m}$), production of electron beams with low momentum spread and good pulse-to-pulse energy stability requires femtosecond electron bunches to be injected with femtosecond synchronization with respect to the plasma wake. Although conventional electron sources (photocathode or thermionic RF guns) have achieved subpicosecond electron bunches [4], the requirements for injection into plasma-based accelerators are currently beyond the performance of these conventional electron sources.

Optical injection schemes which rely on laser triggered injection of plasma electrons into a plasma wake have been proposed [5,6] to generate the required femtosecond electron bunches. One method [6,7] utilizes two laser pulses which propagate perpendicular to one another. One (injection) laser pulse intersects the plasma wake generated by the other (drive) laser pulse. The ponderomotive force due to the transverse gradient in the laser intensity of the injection laser pulse accelerates a fraction of the plasma electrons and allows them to be trapped by the plasma wake. One disadvantage of this method of dephasing background electrons is the high laser intensities ($>10^{18}$ W/cm^2) required in the two laser pulses. Consequently, large space charge waves are excited by the injection laser pulse which further complicates the injection process [7].

Recently a new optical injection scheme was proposed [5] which uses three short laser pulses, namely two low intensity injection laser pulses and a pump laser pulse for plasma wake excitation. The pump laser pulse generates a plasma wake through its ponderomotive force, as in the standard laser wake-field accelerator [3]. The two injection laser pulses, one pulse propagating in the forward direction behind the pump laser pulse and the other pulse counterpropagating to the pump laser pulse, collide at a predetermined phase of the plasma wake. During this collision, the beating of the injection laser pulses generates a beat wave that kicks a subset of the background plasma electrons. Under appropriate conditions, described in this paper, some of the background plasma electrons attain sufficient momentum and phase shift to be trapped by the plasma wake.

The trapping mechanism of this colliding laser pulse scheme is somewhat analogous to the self-trapping process that can occur in the self-modulated laser wake-field accelerator [8]. Self-trapped electrons with energies as high as 100 MeV have been observed in recent experiments [9–13]. In addition to producing a large wake field via self-modulation, a long pulse laser ($L > \lambda_p$, where L is the laser pulse length) decays into Raman backscattered light and a plasma wave [3]. The backscattered light can beat with the pump pulse, generating a slow phase velocity beat wave, and accelerating background plasma electrons to sufficient energies so as to be trapped by the plasma wake [8]. The drawback of using self-modulation of the pump pulse as an electron source is that it produces electron bunches with near 100% energy spread. This is the case since the slow beat wave is not localized with respect to the phase of the plasma wave (i.e., the beat wave extends over distances much larger than the plasma wavelength). Furthermore, self-modulation relies on

 ©1999 The American Physical Society

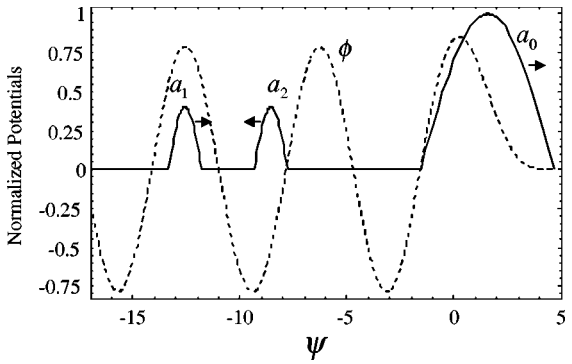

FIG. 1. Normalized potential profiles of the pump laser pulse a_0, the plasma wake ϕ, forward injection laser pulse a_1, and the backward injection laser pulse a_2.

instabilities, i.e., trapping and acceleration occur in an uncontrolled manner.

The colliding laser pulse scheme [5] has the potential to produce femtosecond electron bunches with low fractional energy spreads ($\sim 1\%$) using relatively low injection laser pulse intensities compared to the pump laser pulse $a_{\rm inj}^2 \ll a_{\rm pump}^2 \sim 1$, where $a = eA/mc^2 \simeq 8.5\times 10^{-10}[\lambda(\mu{\rm m})][I^{1/2}({\rm W/cm^2})]$ is the normalized vector potential, I is the laser pulse intensity, and λ is the laser wavelength. Note that since $L \lesssim \lambda_p$ for the three laser pulses considered in this scheme, Raman instabilities will be suppressed. The colliding pulse concept also offers detailed control of the injection process. The injection phase is determined by the relative timing between the forward propagating injection laser pulse and the pump laser pulse. The beat wave phase velocity is adjusted by varying the frequency detuning between the injection laser pulses, and the number of trapped electrons can be controlled by the injection laser pulse intensities and durations.

In this paper we systematically explore the colliding laser pulse optical injection scheme. In Sec. II we calculate the threshold laser pulse amplitudes and the optimal injection wake phase for trapping using a Hamiltonian approach. In Sec. III we present numerical simulation results from a three-dimensional particle transport code which verify the analytic predictions and are used to characterize the dynamics and quality of the generated electron bunches. Conclusions are offered in Sec. IV. A calculation of the trapping volume is presented in Appendix A and in Appendix B we calculate the longitudinal dynamics of the trapped electron bunches.

II. PHASE SPACE ANALYSIS

The colliding laser pulse optical injection scheme employs three short laser pulses as shown in Fig. 1: an intense ($a_0^2 \lesssim 1$) laser pulse (denoted by subscript 0) for plasma wake generation, a forward propagating injection laser pulse (subscript 1), and a backward propagating injection laser pulse (subscript 2). The pump laser pulse generates a plasma wake with phase velocity near the speed of light $v_\varphi \simeq c$. The injection laser pulses collide some distance behind the pump laser pulse. When the injection laser pulses collide, they generate a beat wave with a phase velocity $v_b = \Delta\omega/\Delta k \simeq \Delta\omega/2k_0$, where the frequency difference of the injection laser pulses is $\Delta\omega = \omega_1 - \omega_2$ and the wave-number difference is $\Delta k = k_1 - k_2 \simeq 2k_0$ with $k_1 \simeq |k_2| \simeq k_0$. During the time when the two injection laser pulses overlap, the slow beat wave injects plasma electrons into the fast plasma wake for acceleration to high energies.

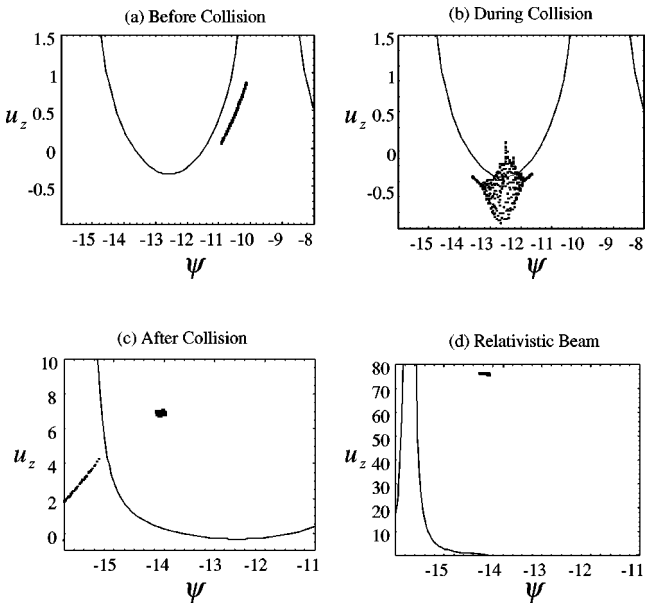

FIG. 2. Electron distribution in longitudinal phase space (ψ, u_z) (a) before the collision of injection laser pulses ($\omega_p t = 36$), (b) during the collision of injection laser pulses ($\omega_p t = 39$), (c) just after the collision ($\omega_p t = 50$), and (d) an energetic electron beam much after the collision ($\omega_p t = 150$). The separatrix between trapped and untrapped plasma wake orbits (solid line) is shown.

An example of the colliding laser pulse injection process is given in Fig. 2, which shows simulation results of the evolution in longitudinal phase space of an initially uniform segment of electrons as they interact with the plasma wake and the beating injection laser pulses. This figure was generated using a particle transport code described in Sec. III. Also shown is the separatrix (solid line) between the trapped and untrapped orbits of the plasma wake Hamiltonian. Figure 2 shows the electron distribution (a) before the collision of the injection laser pulses (in an untrapped orbit of the plasma wake), (b) during the collision of the injection laser pulses (crossing the wake separatrix), (c) just after the collision (0.07 mm of propagation after the collision), and (d) the resulting energetic electron bunch (0.7 mm of propagation after the collision).

A. Plasma wake Hamiltonian

The colliding laser pulse injection mechanism can be studied using a Hamiltonian approach. The electron motion in a one-dimensional (1D) plasma wake is described by the Hamiltonian [14]

$$H(u_z, \psi) = [1 + u_z^2]^{1/2} - \beta_\varphi u_z - \phi(\psi), \tag{1}$$

where $u_z m_e c$ is the electron axial momentum and $c\beta_\varphi$ is the plasma wake phase velocity, which is near the group velocity of the pump laser pulse $v_g \simeq c\beta_\varphi$. The scalar potential of the plasma wake is assumed to have the form $\phi(\psi) = \phi_o \cos\psi$, where the wake phase is $\psi = \omega_p(\beta_\varphi^{-1} z/c - t)$ and the normalized wake potential amplitude is $\phi_o = e\Phi_o/m_e c^2$. The am-

plitude of the wake potential is determined by the pump laser pulse amplitude and shape. The normalized axial momentum of the electron in an orbit $H=$const of the plasma wake is

$$u_z=\beta_\varphi\gamma_\varphi^2[H+\phi(\psi)]\pm\gamma_\varphi\{\gamma_\varphi^2[H+\phi(\psi)]^2-1\}^{1/2}, \quad (2)$$

where $\gamma_\varphi=(1-\beta_\varphi^2)^{-1/2}$. The boundary between trapped and untrapped orbits is given by the separatrix orbit $H=H(u_z=\gamma_\varphi\beta_\varphi,\psi=\pi)=\gamma_\varphi^{-1}+\phi_o$. Assuming the plasma is initially cold, the background electron fluid motion in the plasma wake is defined by the orbit $H=1$.

The 1D Hamiltonian Eq. (1) neglects the effects of transverse focusing. A three-dimensional (3D) plasma wake will have a periodic radial field which is $\pi/2$ out of phase with the accelerating field. Therefore there exists a $\pi/4$ region in wake phase where the fields due to the plasma wake are both focusing and accelerating. For an electron to be trapped and remain in this region where the transverse electric field due to the plasma wake will provide a focusing force, it must be in an orbit defined by $H\leqslant H(u_z=\gamma_\varphi\beta_\varphi,\psi=\pi/2)=\gamma_\varphi^{-1}$.

B. Beat wave Hamiltonian

The colliding injection laser pulses lead to the formation of a beat wave with phase space buckets (separatrices) of width $2\pi/\Delta k\simeq\lambda_0/2$ (much shorter than those of the wake field λ_p, i.e., $\lambda_0\ll\lambda_p$ is assumed). The motion of the electron in the beat wave is described by the beat wave Hamiltonian

$$H_b(u_z,\psi_b)=[\gamma_\perp^2(\psi_b)+u_z^2]^{1/2}-\beta_b u_z, \quad (3)$$

where $\beta_b=\Delta\omega/c\Delta k\simeq(\lambda_2-\lambda_1)/(\lambda_2+\lambda_1)$ is the beat wave phase velocity, $\psi_b=\Delta k(z-\beta_b ct)$ is the beat wave phase, and $\gamma_\perp^2(\psi_b)=1+\hat{a}_1^2+\hat{a}_2^2+2\hat{a}_1\hat{a}_2\cos\psi_b$ with $\hat{a}_1^2$ and $\hat{a}_2^2$ the slowly varying amplitudes of the forward and backward injection laser pulses averaged over the rapid phase oscillations. The separatrix orbit in phase space of the beat wave Hamiltonian has the value $H_b=H_b(u_z=\gamma_b\beta_b\gamma_\perp(0),\psi_b=0)=\gamma_\perp(0)\gamma_b^{-1}$, where $\gamma_b=(1-\beta_b^2)^{-1/2}$. The maximum $(+)$ and minimum $(-)$ normalized axial momenta of an electron in a beat wave orbit (extrema of the separatrix) are

$$u_{\text{beat}}=\gamma_b\beta_b\gamma_\perp(0)\pm2\gamma_b(\hat{a}_1\hat{a}_2)^{1/2}. \quad (4)$$

As we will show, the beat wave amplitude parameter $(\hat{a}_1\hat{a}_2)^{1/2}$ is a critical parameter in the injection process. For $\hat{a}_1=\hat{a}_2=\hat{a}_{\text{inj}}$ the beat wave amplitude parameter $(\hat{a}_1\hat{a}_2)^{1/2}=\hat{a}_{\text{inj}}=eE_{\text{inj}}/m_ec\omega_{\text{inj}}$ is the normalized root-mean-squared (rms), averaged over a laser period, electric field amplitude of the injection laser pulses.

Since the transit time of an untrapped electron through a beat wave orbit and the bounce time of a deeply trapped electron in a beat wave orbit are both much shorter than a plasma wave period, a separation of time scales is possible. This discrepancy in time scales is due to the extremely small spatial scale $\lambda_0/2$ of the beat wave orbits in comparison to the plasma wake orbit λ_p. It can be shown that the bounce period for an electron deeply trapped in the beat wave is given by $\tau_b=(2\pi/c\Delta k)\gamma_b^2\gamma_\perp(\pi)/(\hat{a}_1\hat{a}_2)^{1/2}$. This bounce time is typically much shorter than the transit time $\sim\lambda_p/c$ of a plasma electron through a single period of the plasma wake. Therefore, on the time scale in which a single electron interacts with a beat wave orbit, it can be assumed that the electron experiences a constant electric field from the plasma wake. The effect of the plasma wake electric field on the phase space orbits is to distort the beat wave orbits.

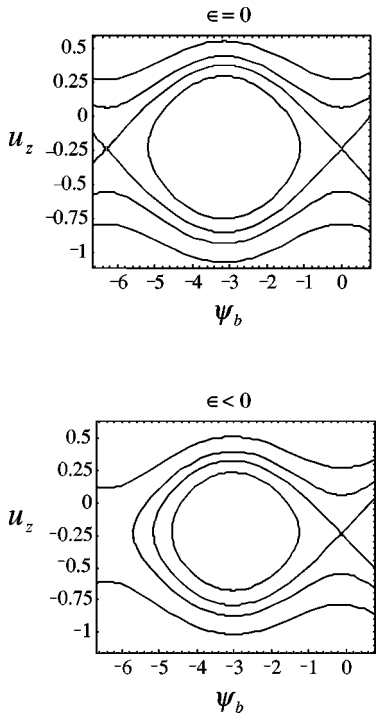

FIG. 3. Distortion of the beat wave orbits in phase space (ψ_b,u_z) due to the presence of the plasma wake $\epsilon=eE_z(\psi_o)/(m_ec^2\Delta k)$. With $\epsilon<0$, the buckets open to the right allowing electrons moving along untrapped orbits to be trapped by the plasma wake.

About a single period of the beat wave, the plasma wake electric field $E_z=-(m_ec^2/e)(\partial/\partial z)\phi$ can be approximated as a constant [i.e., for small phase excursions $\psi\ll2\pi$ about ψ_o, $E_z(\psi)\simeq E_z(\psi_o)$, where ψ_o is the local wake phase position of the beat wave bucket and $E_z(\psi_o)$ is the local value of the plasma wake axial electric field]. The beat wave Hamiltonian Eq. (3) will be modified due to the presence of $E_z(\psi_o)$,

$$H_b(u_z,\psi_b)=[\gamma_\perp^2(\psi_b)+u_z^2]^{1/2}-\beta_b u_z+\epsilon\psi_b, \quad (5)$$

where $\epsilon=eE_z(\psi_o)/(m_ec^2\Delta k)$ is constant.

Equation (5) describes the distortion of the (u_z,ψ_b) phase space from symmetric islands $(\epsilon=0)$ to ''fish-shaped'' islands $(\epsilon\neq0)$ as shown in Fig. 3. When $\epsilon=0$, the separatrix is symmetric in ψ_b about the stable fixed point (o point), e.g., located at $\psi_b=-\pi$, with unstable fixed points (x points) located at $\psi_b=0,-2\pi$. When $\epsilon\neq0$, the separatrix is fish-shaped and the enclosed region of phase space is reduced (compared with $\epsilon=0$) and lies inside the region $-2\pi<\psi_b<0$. For example, when $\epsilon<0$, the ''fish-tail'' of the separatrix opens to the right, i.e., the x point lies to the left of $\psi_b=0$. In the limit $\pi|\epsilon|\gamma_b\gamma_\perp(0)/2\hat{a}_0\hat{a}_1<1$, the maximum and minimum axial momenta for an electron on the separatrix are

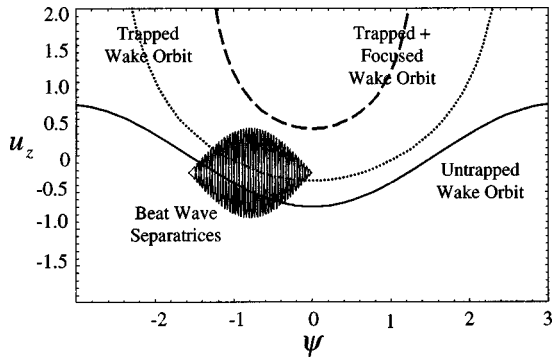

FIG. 4. Phase space (ψ,u_z) showing the beat wave separatrices, an untrapped plasma wake orbit (solid line), a trapped plasma wake orbit (dotted line), and a trapped and focused plasma wake orbit (dashed line).

$$u_{\rm beat} \simeq \beta_b \gamma_b [\gamma_\perp(0) - \pi|\epsilon|\gamma_b] \pm 2\gamma_b(\hat{a}_0\hat{a}_1)^{1/2}\left(1 - \frac{\pi|\epsilon|\gamma_b\gamma_\perp(0)}{2\hat{a}_0\hat{a}_1}\right)^{1/2}. \quad (6)$$

Both the width and height of the separatrix decrease with increasing $|\epsilon|$.

The electron fluid momentum in the plasma wake is given by Eq. (2) with $H=1$. For $\gamma_\varphi^2 \gg 1$, the normalized electron fluid momentum is $u_z \simeq -\phi_0 \cos(\psi)\{[1+\phi_0\cos(\psi)/2]/[1+\phi_0\cos(\psi)]\}$. Trapping may occur by the following method. In the region $-\pi/2<\psi<0$, the plasma electrons are flowing backward $(u_z<0)$ and the electric field is accelerating $(E_z<0)$. If $E_z<0$, then $\epsilon<0$ and the beat wave orbits open to the right, as shown in Fig. 3. Consider an electron initially flowing backward, as it would in the region $-\pi/2<\psi<0$, thus initially residing below the beat wave separatrix. As Fig. 3 indicates, the orbits are open and can take an electron from below to above the beat wave separatrix. Such an electron would acquire a positive axial momentum which is sufficiently high to be trapped and accelerated by the plasma wake. The open phase space orbits provide a possible path by which the ponderomotive beat wave can lead to trapping of electrons in the plasma wake.

C. Trapping threshold

The threshold injection laser pulse intensities required for trapping of background plasma electrons into the plasma wake can be estimated by considering the effects of the plasma wake and the beat wave individually and requiring resonance overlap (shown in Fig. 4). Specifically, the maximum momentum of the beat wave separatrix exceeds the minimum momentum of the plasma wake separatrix and the minimum momentum of the beat wave separatrix is less than the fluid momentum of electrons in the plasma wake. With these requirements, the necessary conditions for trapping are

$$(u_{\rm beat})_{\rm max} \geqslant u_{\rm trap}, \quad (7)$$

$$(u_{\rm beat})_{\rm min} \leqslant u_{\rm untrap}. \quad (8)$$

The maximum and minimum momenta of an electron in a beat wave orbit are given in Eq. (4). The momentum of a plasma electron in an untrapped orbit of the plasma wake $u_{\rm untrap}$ is given by Eq. (2) with $H=1$ (i.e., the background plasma fluid electrons). The momentum of an electron in a trapped orbit of the plasma wake $u_{\rm trap}$ is given by Eq. (2) with $H \leqslant \gamma_\varphi^{-1} + \phi_o$. For an electron in a trapped and focused orbit, $u_{\rm trap}$ is given by Eq. (2) with $H \leqslant \gamma_\varphi^{-1}$.

Solving for the minimum $(\hat{a}_1\hat{a}_2)^{1/2}$ which satisfies the conditions Eqs. (7) and (8) yields the threshold beat wave amplitude parameter for trapping plasma electrons,

$$(\hat{a}_1\hat{a}_2)_{\rm th}^{1/2} = \frac{1-H}{4\gamma_b(\beta_\varphi - \beta_b)}, \quad (9)$$

and the optimal wake phase for injection [location in wake phase of the threshold beat wave amplitude parameter Eq. (9)],

$$\cos\psi_{\rm opt} = \phi_o^{-1}\left[\gamma_b(1-\beta_\varphi\beta_b)\gamma_\perp(0) - \frac{1}{2}(1+H)\right]. \quad (10)$$

Here $H=\gamma_\varphi^{-1}+\phi_o$ for injection into a trapped plasma wake orbit and $H=\gamma_\varphi^{-1}$ for injection into a trapped and focused plasma wake orbit. In the limit $\gamma_\varphi^2 \gg 1$, $\beta_b \ll 1$, and $\hat{a}_i^2 \ll 1$, Eqs. (9) and (10) become $4(\hat{a}_1\hat{a}_2)_{\rm th}^{1/2} \simeq (1+\beta_b)(1-H)$ and $2\phi_o\cos\psi_{\rm opt} \simeq 1-2\beta_b-H$ with $H \simeq \phi_o$ for a trapped orbit and $H \simeq 0$ for a trapped and focused orbit. As an example, the parameters $\beta_b=-0.2$, $\gamma_\varphi=50$, and $\phi_o=0.7$ give a threshold of $(\hat{a}_1\hat{a}_2)_{\rm th}^{1/2} \simeq 0.2$ and an optimal injection phase of $\psi_{\rm opt} \simeq 0$ for injection into a trapped and focused orbit. A calculation of the wake phase region where trapping is possible for given injection laser pulse amplitudes is provided in Appendix A.

Figure 5(a) shows the threshold beat wave amplitude parameter for trapping [Eq. (9) with $H=\gamma_\varphi^{-1}+\phi_o$] and Fig. 5(b) shows the optimal wake phase for injection versus the beat wave phase velocity β_b for several wake potential amplitudes. From Fig. 5(a) one sees that the larger the plasma wake, the smaller the injection laser pulse intensity required for trapping plasma electrons. The threshold for injection into a trapped and focused orbit is independent of plasma wake amplitude as indicated by Eq. (9) with $H=\gamma_\varphi^{-1}$. In the limit $\gamma_\varphi^2 \gg 1$, the threshold beat wave amplitude parameter for a trapped and focused orbit is $(\hat{a}_1\hat{a}_2)^{1/2} \simeq 1/[4\gamma_b(1-\beta_b)] \leqslant 0.25$ for $\beta_b \leqslant 0$. Figure 5(a) also shows that the threshold slightly decreases for decreasing β_b. Note that the estimate of the trapping threshold Eq. (9) will not be valid when the separation in time scales no longer applies (i.e., when $|\beta_b|$ is large enough such that $\tau_b \sim \lambda_p/c$). Furthermore, validity of Eq. (10) requires $|\cos\psi_{\rm opt}|<1$.

Minimizing the injection pulse amplitudes [operating near the threshold amplitude given by Eq. (9)] will minimize the laser power $P_i \simeq 43(\hat{a}_i r_i/\lambda_i)^2$ GW required for trapping and is therefore important for the experimental realization of this injection scheme. For illustration, if the injection laser pulses have a wavelength of 0.8 μm and a spot size of 15 μm, then the injection laser pulse power required for trapping is $P_i \leqslant 1$ TW for $\hat{a}_i \leqslant 0.26$.

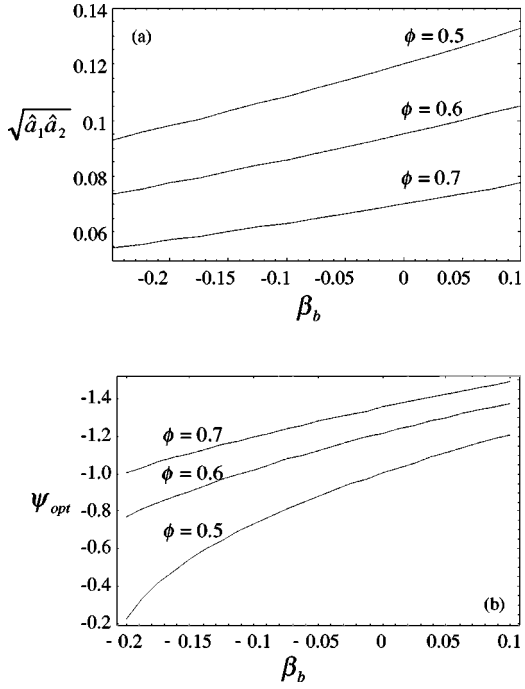

FIG. 5. (a) The threshold beat wave amplitude parameter $(\hat{a}_1\hat{a}_2)^{1/2}$ for trapping at the optimal injection phase [Eq. (9)] versus beat wave phase velocity (for $\phi_o = 0.5$, 0.6, and 0.7). (b) The optimal wake phase for injection $\psi_{\rm opt}$ [Eq. (10)] versus beat wave phase velocity (for $\phi_o = 0.5$, 0.6, and 0.7).

III. NUMERICAL STUDIES

To further evaluate the colliding laser pulse scheme and to test the analytic predictions for the trapping thresholds presented in Sec. II, the motion of test particles in the combined plasma wake and laser fields was simulated by numerically solving the equations of motion for the electrons (relativistic Lorentz equation). In the numerical simulations, we assume the laser pulses are linearly polarized with fundamental Gaussian radial profiles and half-period cosine longitudinal envelopes. In the paraxial approximation ($\lambda_i \ll r_{si}$, where λ_i is the laser wavelength and r_{si} is the minimum laser spot size) the normalized vector potential of the laser pulses is $\vec{a}_i = \hat{e}_{\perp i} a_{\perp i} + \hat{e}_z a_{zi}$ where $\hat{e}_{\perp i}$ and $\hat{e}_z$ are unit vectors and the vector potential components are given by [15]

$$a_{\perp i} = \sqrt{2}\hat{a}_i \frac{r_{si}}{w_i} \exp[-r^2/w_i^2] \cos\psi_i , \tag{11}$$

$$a_{zi} = 2\sqrt{2}\hat{a}_i \frac{(\vec{x}\cdot\hat{e}_{\perp i}) r_{si}}{k_i w_i^3} \exp[-r^2/w_i^2] \times [\sin\psi_i - (z/Z_{Ri})\cos\psi_i]. \tag{12}$$

Here $\omega_i = 2\pi c/\lambda_i$ is the laser frequency, $w_i(z) = r_{si}(1 + z^2/Z_{Ri}^2)^{1/2}$ is the laser spot size, $Z_{Ri} = k_i r_{si}^2/2$ is the Rayleigh length, and $\psi_i = k_i(z - \beta_{\varphi i} ct) + z r^2/(w_i^2 Z_{Ri}) + z/Z_{Ri} - \tan^{-1}(z/Z_{Ri}) + \varphi_i$ is the phase with φ_i a constant. The phase velocity $c\beta_{\varphi i} = \omega_i/k_i$ and group velocity $c\beta_{gi}$ are given by $\beta_{\varphi i}^{-1} = \beta_{gi} = \pm(1 - \omega_p^2/\omega_i^2 - 4c^2/r_{si}^2\omega_i^2)^{1/2}$. The positive sign is taken for the pump laser pulse and forward propagating injection laser pulse and the negative sign is taken for the backward propagating injection laser pulse. The longitudinal profile of the pump pulse is assumed to have the form $\hat{a}_0 = -a_0 \Pi((2\psi - \pi)/4\pi)\cos[(2\psi - \pi)/4]$, where $\Pi(s)$ is a step function such that $\Pi(s) = 1$ for $|s| < 1/2$ and zero otherwise. The injection laser pulses are assumed to have longitudinal profiles of the form $\hat{a}_i = a_i \Pi(s_i)\cos(\pi s_i)$, where $s_i = (z - \beta_{gi} ct - z_i) L_i^{-1}$ with L_i the length of the injection laser pulses and z_i a constant.

The polarizations of the laser pulses are chosen to be $\hat{e}_{\perp 0} = \hat{x}$ and $\hat{e}_{\perp 1} = \hat{e}_{\perp 2} = \hat{y}$ such that $\vec{a}_0 \cdot \vec{a}_2 \simeq 0$ and thus there is no beating (no slow wave generation) from the interaction of the pump laser pulse and the counterpropagating injection laser pulse. The ponderomotive potential due to the beating of the injection laser pulses (averaged over the fast phase oscillations) is $\vec{a}_1 \cdot \vec{a}_2 = \hat{a}_1^2 + \hat{a}_2^2 + 2\hat{a}_1\hat{a}_2 \cos(\psi_1 - \psi_2)$. The plasma wake fields produced by the injection laser pulses can be neglected ($\phi_1 \sim \phi_2 \ll \phi_0$) since the injection laser pulse amplitudes required for trapping are much less than the pump laser pulse amplitude and the pulse lengths of the injection laser pulses can be chosen to provide poor coupling between the plasma response and the injection laser pulses.

Assuming $a_0^2 < 1$, the plasma wake potential ϕ excited by the ponderomotive force generated by the pump laser pulse (to lowest order in pump laser pulse amplitude) near the waist of the pump laser pulse ($z \ll Z_{R0}$) satisfies [16]

$$\phi = \frac{\hat{a}_0^2}{4} \exp[-2r^2/r_{s0}^2] \left[1 + \sin\psi + \left(\frac{3\pi}{4} - \frac{\psi}{2} \right) \cos\psi \right] \tag{13}$$

inside the pump laser pulse, and

$$\phi = \frac{\pi \hat{a}_0^2}{4} \exp[-2r^2/r_{s0}^2] \cos\psi \tag{14}$$

after the pump laser pulse. The axial and radial components of the electric field due to the plasma wake potential after the pump laser pulse are

$$E_z = \frac{m_e c^2}{e} \frac{\omega_p}{c} \phi_0 \exp[-2r^2/r_{s0}^2] \sin\psi, \tag{15}$$

$$E_r = \frac{m_e c^2}{e} \frac{4r}{r_{s0}^2} \phi_0 \exp[-2r^2/r_{s0}^2] \cos\psi, \tag{16}$$

where $\phi_o = \pi \hat{a}_0^2/4$. The radial electric field will provide a focusing force for an electron at a plasma wake phase of $\cos\psi > 0$ and a defocusing force for $\cos\psi < 0$, as noted in Sec. II A.

The equations of motion (relativistic Lorentz equation) for the plasma electrons in the combined 3D fields of the three lasers and the plasma wake were numerically integrated using an adaptive step-size Runge-Kutta method [17]. The plasma was assumed to be initially homogeneous and cold such that the test particles were loaded uniformly with no initial momentum. Unless otherwise stated, the parameters used in the numerical simulations are listed in Table I.

TABLE I. Simulation parameters.

Plasma wavelength λ_p	40 μm
Pump laser strength $\hat{a}_0$	0.94
Plasma wake potential ϕ_o	0.7
Pump pulse length $L_0=\lambda_p$	40 μm
Pump pulse wavelength λ_0	0.8 μm
Laser spot size $r_{s0}=r_{s1}=r_{s2}$	15 μm
Injection laser pulse strength $\hat{a}_1=\hat{a}_2$	0.4
Injection pulse length $L_1=L_2=\lambda_p/2$	20 μm
Injection pulse (forward) wavelength λ_1	0.83 μm
Injection pulse (backward) wavelength λ_2	0.80 μm

A. Simulation results

The orbit of a single test electron in longitudinal phase space (ψ,u_z) interacting with the combined fields of the lasers and the plasma wake is shown in Fig. 6. The dotted line shows the separatrix between trapped and untrapped orbits of the plasma wake Hamiltonian Eq. (1), the dashed line shows the orbit of the test electron without the beating injection laser pulses (following an untrapped plasma wake orbit), and the solid line shows the orbit of the test electron interacting with the beating injection laser pulses. Figure 6 shows the phase shift and momentum gain from the beating injection laser pulses allowing the test electron to move from an untrapped to a trapped plasma wake orbit.

The particle transport code was used to test the analytic predictions made by the Hamiltonian analysis of the motion of electrons in the beat wave and the plasma wake presented in Sec. II. The minimum injection laser pulse amplitude for injection of plasma electrons into a trapped orbit of the plasma wake is shown in Fig. 7(a). The solid line is the analytic estimation, Eq. (9), with $H=\gamma_\varphi^{-1}+\phi_o$ and $\beta_\varphi=-0.2$, and the points correspond to simulation results. A somewhat higher ($\sim$10%) laser pulse amplitude is needed for trapping in the simulation results than predicted by the analytic estimation. This is due to the nonconstant laser pulse profiles (longitudinal and transverse) used in the numerical simulations [i.e., the electrons experience a lower $(\hat{a}_1\hat{a}_2)^{1/2}$ before and after the collision of the maxima of the injection laser pulses and when the particles move off axis due to the transverse fields of the plasma wake].

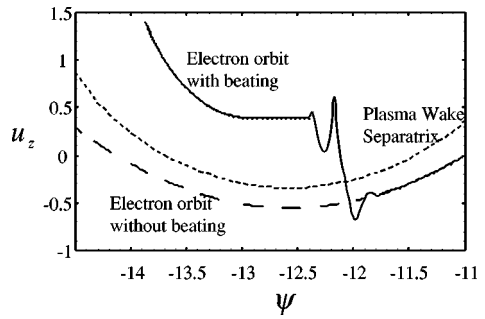

FIG. 6. Phase space (ψ,u_z) orbit of test electron without the beating injection laser pulses (dashed line) and with the test electron experiencing the influence of the beating injection laser pulses (solid line). The separatrix between trapped and untrapped plasma wake orbits (dotted line) is shown.

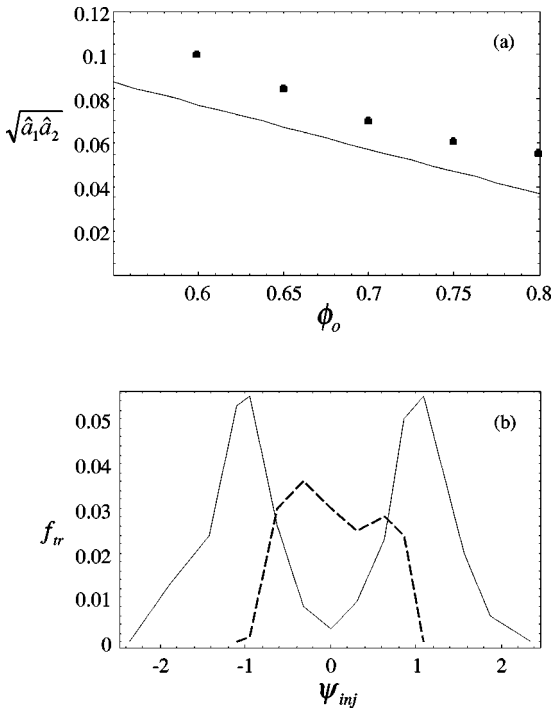

FIG. 7. (a) Threshold beat wave amplitude parameter $(\hat{a}_1\hat{a}_2)^{1/2}$ versus plasma wake potential amplitude. Solid line is Eq. (9) with $\phi_o=0.7$ and $\beta_b=-0.2$. Points are numerical simulation results. (b) Fraction of loaded test electrons which become trapped and focused (dashed line) and the fraction of loaded test electrons which become trapped and defocused (solid line) after the colliding laser pulses versus injection wake phase $\psi_{\rm inj}$.

To determine the optimal injection wake phase which minimizes the injection laser pulse amplitude required for trapping of background plasma electrons, the fraction of loaded test electrons which become trapped $f_{\rm tr}$ as a result of the colliding injection laser pulses was examined as a function of the injection wake phase (the plasma wake phase where the maxima of the injection laser pulses collide). Figure 7(b) shows the fraction of loaded electrons which become trapped and focused (dashed line) and the fraction which become trapped and defocused (solid line) versus the injection wake phase $\psi_{\rm inj}$. In Fig. 7(b), $f_{\rm tr}$ is defined as the fraction of electrons that become trapped which were loaded uniformly in a region of length $\pi/2$ in wake phase about $\psi_{\rm inj}$ and $r\leqslant 2$ μm (simulations show electrons loaded with $r>2$ μm do not become trapped). The trapping fraction is peaked at $\psi_{\rm opt}\simeq\pm 1.0$, which agrees well with the analytic predictions [Eq. (10) with $\beta_b=-0.2$ and $\phi_o=0.7$]. The asymmetry in the trapping fraction shown in Fig. 7(b) is due to the distortion of the beat wave buckets from the presence of the plasma wake as described in Sec. II B. Significant trapping of electrons occurs in an injection wake phase region of $-1.5\lesssim\psi_{\rm inj}\lesssim 1.5$. This indicates that the two colliding injection laser pulses must be synchronized to the plasma wake with an accuracy of $\sim$10 fs, which is not a serious timing constraint for current laser technology.

B. Electron bunch dynamics

To further characterize the performance of this optical injection concept, the dynamics of the trapped electron

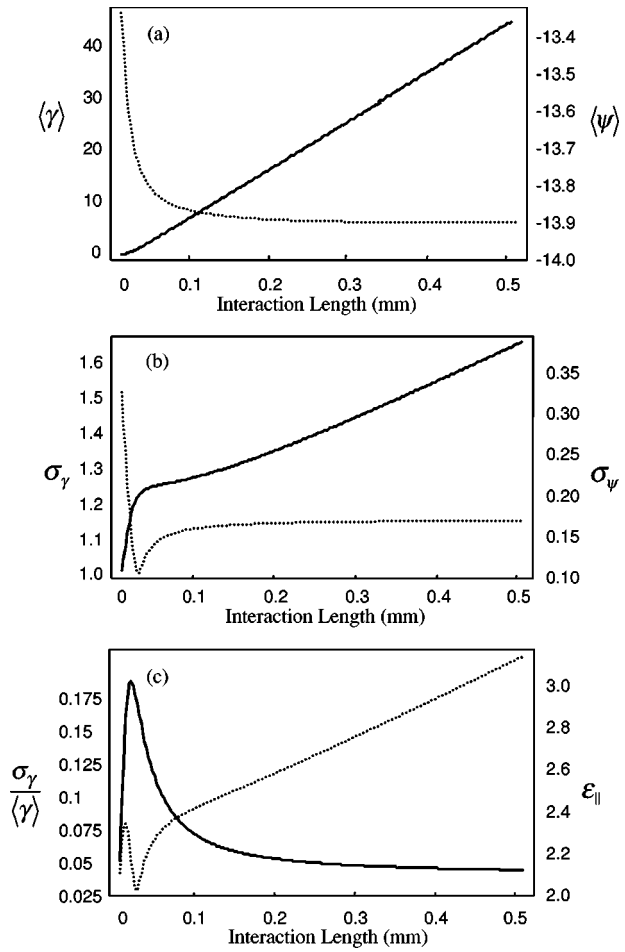

FIG. 8. Dynamics of trapped electron bunch. (a) The mean phase $\langle\psi\rangle$ (dashed line) and mean energy $\langle\gamma\rangle$ (solid line) of a trapped electron bunch versus interaction length. (b) The rms phase spread σ_ψ (dashed line) and rms energy spread σ_γ (solid line) of a trapped electron bunch versus interaction length. (c) Fractional energy spread $\sigma_\gamma/\langle\gamma\rangle$ (solid line) and longitudinal rms emittance $\varepsilon_\parallel(10^{-9}$ eV sec) (dashed line) of a trapped electron bunch versus interaction length.

bunches were studied analytically and numerically. In Appendix B we calculate the longitudinal dynamics of a relativistic electron bunch trapped in the plasma wake. Figure 8 shows an example of simulation results of the evolution of a typical trapped and focused electron bunch generated by colliding the injection laser pulses at a wake phase of $\psi_{\rm inj}=0$.

The mean phase $\langle\psi\rangle$ (dashed line) and mean energy $\langle\gamma\rangle$ (solid line) of a trapped electron bunch versus interaction length are shown in Fig. 8(a). The interaction length $L_{\rm int}$ considered in these simulations is much less than the dephasing length $L_{\rm int}\ll L_{\rm dephase}\sim\lambda_p\gamma_\varphi^2$ (i.e., interaction times much shorter than the bounce time in a trapped plasma wake orbit) and less than the Rayleigh length $L_{\rm int}<Z_{R0}$. The figure shows the reduction of phase slippage as the bunch becomes relativistic and the linear growth of the mean energy of the bunch in this regime. The rms phase spread σ_ψ (dashed line) and the rms energy spread σ_γ (solid line) of the trapped electron bunch versus interaction length are plotted in Fig. 8(b). Figure 8(b) shows the rms phase spread (or bunch duration, which is defined as $\omega_p^{-1}\sigma_\psi$) is constant once the bunch becomes relativistic due to the absence of phase slippage for the interaction lengths considered [$\delta\psi=(\beta_z-\beta_\varphi)\omega_p\delta t\approx 0$ for $c\,\delta t\ll\lambda_p\gamma_\varphi^2$]. Figure 8(c) shows the fractional energy spread $\sigma_\gamma/\langle\gamma\rangle$ (solid line) and the longitudinal rms emittance (dashed line) of the trapped electron bunch versus interaction length. The longitudinal rms emittance is defined as $\varepsilon_\parallel$ (eV sec)$=m_ec^2\omega_p^{-1}(\sigma_\gamma^2\sigma_\psi^2-\sigma_{\gamma\psi}^2)^{1/2}$, where $\sigma_{\gamma\psi}=\langle\gamma\psi\rangle-\langle\gamma\rangle\langle\psi\rangle$. As Fig. 8(c) indicates, the longitudinal rms emittance is not conserved and the fractional energy spread of a trapped electron bunch asymptotes to a constant value. A calculation of the asymptotic value of the fractional energy spread Eq. (B12) is provided in Appendix B. The longitudinal rms emittance is not conserved since the bunch becomes highly relativistic at a wake phase where the axial electric field Eq. (15) is a nonlinear function of wake phase.

Near the axis $r/r_{s0}<1$, the radial electric field of the plasma wake Eq. (16) is linear with respect to the radial coordinate to lowest order in $O(r/r_{s0})$. If the electron bunch is injected into the focusing region ($\cos\psi>0$), the radial electric field will provide a focusing force with a focusing strength $k^2=eE_r/\gamma m_ec^2r\simeq(4\phi_o/\gamma r_{s0}^2)\cos\psi$. The evolution of the rms radius of the electron bunch will be described by the envelope equation [18]

$$\sigma_r''+\frac{\gamma'}{\gamma}\sigma_r'+k^2\sigma_r=\frac{2(I/I_A)}{\gamma^2\sigma_r}+\frac{\varepsilon_\perp^2}{\gamma^2\sigma_r^3},\tag{17}$$

where primes indicate derivatives with respect to ct, $\sigma_r=[\langle r^2\rangle-\langle r\rangle^2]^{1/2}$ is the rms radius of the electron bunch, I is the beam current, $I_A=(m_ec^3/e)\beta\gamma$ is the Alfvén current, and $\varepsilon_\perp=\gamma(\sigma_r^2\sigma_{r'}^2-\sigma_{rr'}^2)^{1/2}$ is the normalized transverse rms emittance where $\sigma_{r'}^2=\langle r'^2\rangle-\langle r'\rangle^2$ and $\sigma_{rr'}=\langle rr'\rangle-\langle r\rangle\langle r'\rangle$. With linear focusing, the normalized transverse rms emittance is conserved for a monoenergetic beam. Figure 9 shows the transverse phase space $(\omega_px/c,\gamma\beta_x)$ of the trapped and focused electron bunch presented in Fig. 2(c) just after the collision of the injection laser pulses (after 0.07 mm of propagation) and in Fig. 2(d) after 0.7 mm of propagation. The slight increase in normalized transverse rms emittance shown in these figures is due to the nonlinear focusing force provided by the plasma wake. In principle, a collimator may be used to spatially filter the trapped bunch and reduce the transverse emittance.

The effects of space charge within the trapped electron bunch were not included in these simulations. This omission can be justified by considering the ratio of space charge to emittance terms in the beam envelope equation Eq. (17),

$$2\frac{I}{I_A}\frac{\sigma_r^2}{\varepsilon_\perp^2}.\tag{18}$$

For the electron bunches described in Sec. III C, the ratio of the space charge term to the emittance term Eq. (18) is $\sim 10^{-3}$, and the bunch is emittance dominated.

Space charge forces should not be a concern longitudinally if the electric field due to space charge forces within the bunch is much less than the axial electric field due to the plasma wake [19]. This will be satisfied when the ratio of beam density n_b to the plasma density n_e is $n_b/n_e\ll a_0^2/\sigma_\psi$, where σ_ψ is the spread in wake phase of the elec-

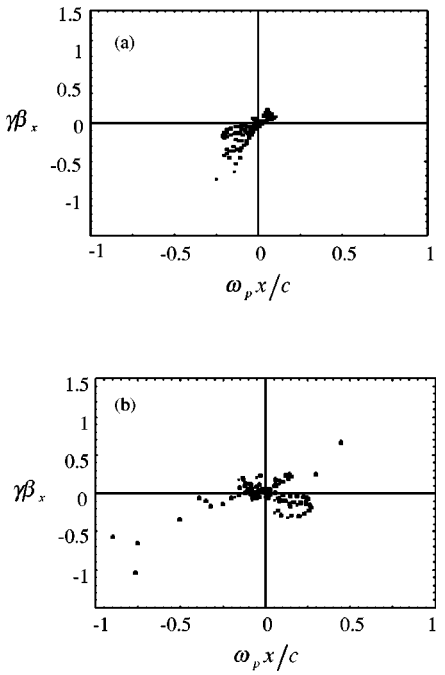

FIG. 9. Transverse phase space distribution $(\omega_p x/c, \gamma\beta_x)$ of a trapped and focused electron bunch (a) just after the collision of the injection laser pulses (after 0.07 mm of propagation) and (b) after 0.7 mm of propagation.

tron bunch. For the parameters under consideration in this paper, this condition is satisfied and the space charge effects are small while the bunch remains in the plasma. Space charge effects can become quite significant after the bunch leaves the plasma.

C. Electron bunch quality

The quality of the electron bunch can be examined as the beat wave amplitude parameter $(\hat{a}_1\hat{a}_2)^{1/2}$ is increased beyond the threshold value for injection into a trapped and focused orbit, Eq. (9), with $H \leqslant \gamma_\varphi^{-1}$. Figure 10(a) shows the fraction of loaded test electrons which become trapped and focused (solid line) as a result of colliding the injection laser pulses at a wake phase of $\psi_{\rm inj}=0$ versus the beat wave amplitude parameter. The fraction of loaded test electrons is defined as in Sec. III A. The maximum value shown on Fig. 10(a) corresponds to a bunch number of $N_b \simeq 0.5\times 10^7$ electrons for a plasma density of $n_e = 7\times 10^{17}$ cm^{-3}.

As shown in Sec. III B, the rms phase spread (bunch duration) is constant for a highly relativistic bunch, the fractional energy spread is asymptotic, and the transverse normalized rms emittance is conserved for large pump laser spot size. Therefore, we examined these three measures of bunch quality versus increasing beat wave amplitude parameter. Figure 10(a) shows the bunch duration of the trapped electron bunch (dashed line) versus the beat wave amplitude parameter. The asymptotic fractional energy spread $\sigma_\gamma/\langle\gamma\rangle$ (solid line) and the normalized transverse rms emittance $\varepsilon_\perp$ (dashed line) after 0.5 mm of propagation versus the beat wave amplitude parameter are shown in Fig. 10(b). These figures indicate the production of ~ 1 fs election bunches with $\sim 1\%$ fractional energy spread and ~ 1 mm mrad normalized transverse rms emittance.

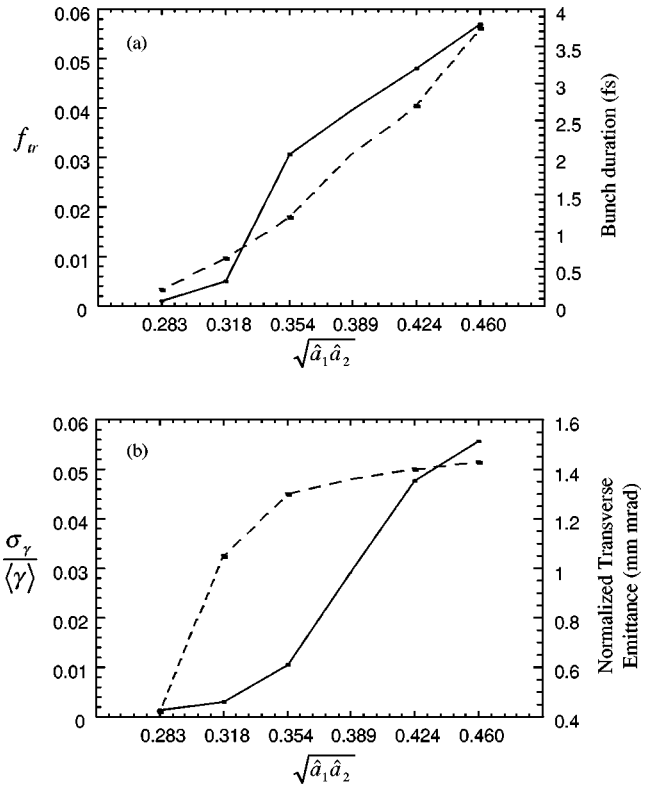

FIG. 10. (a) Fraction of loaded test electrons which become trapped and focused after the colliding laser pulses (solid line) and bunch duration (fs) of trapped electron bunch (dashed line) versus beat wave amplitude parameter. (b) Asymptotic fractional energy spread $\sigma_\gamma/\langle\gamma\rangle$ (solid line) and normalized transverse rms emittance $\varepsilon_\perp$ (mm mrad) (dashed line) after 0.5 mm of propagation of trapped electron bunch versus beat wave amplitude parameter.

A dramatic example of the colliding pulse injection process is shown in Fig. 2 for $L_1 = L_2 = 10$ μm and $\hat{a}_1 = \hat{a}_2 = 0.32$ with $\psi_{\rm inj}=0$ (other parameters as in Table I). Figure 2 shows longitudinal phase space (ψ, u_z) of the test electrons. As shown in Fig. 2(d), the results are very dramatic: a 1 fs electron bunch with energy 39 MeV, fractional energy spread of 0.2%, and normalized transverse emittance $\simeq 0.9$ mm mrad. The bunch number is $N_b \simeq 2.6\times 10^6$ electrons for a plasma density of $n_e = 7\times 10^{17}$ cm^{-3}.

The number of trapped electrons can be increased by increasing the injection laser spot size (i.e., increasing the injection laser pulse power). Figure 11 shows that the number of trapped and focused electrons increases for increasing spot size of the laser pulses (other parameters the same as Fig. 2). For $r_{s0} = r_{s1} = r_{s2} = 30$ μm $(P_1 = P_2 \simeq 6$ TW), the number of trapped electrons increases to $N_b \simeq 14.5\times 10^6$ electrons.

IV. SUMMARY AND DISCUSSION

In this paper, we have explored the generation of ultrashort electron bunches by using colliding laser pulses to dephase background plasma electrons undergoing fluid oscillations in a plasma wake. A variation of this scheme, which relies on the same trapping mechanism, is to remove the forward propagating injection laser pulse and to beat the pump laser pulse with the backward propagating injection laser pulse. Near the back of the pump pulse, a sufficiently

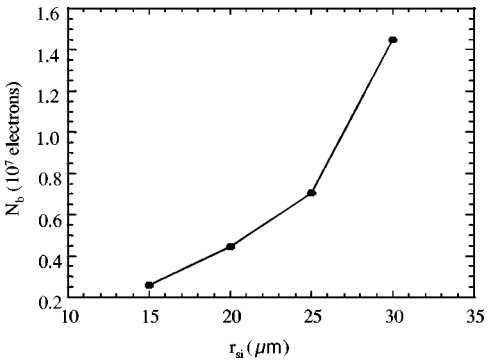

FIG. 11. Number of trapped and focused electrons N_b versus spot size of laser pulses ($r_{s0}=r_{s1}=r_{s2}$).

large plasma wake will be generated to allow trapping of plasma electrons dephased by the slow wave created by the beating of the pump laser pulse and the backward propagating injection laser pulse. Alternatively, colliding pulse injection could be done using several forward propagating injection pulses (which are properly phased) and a single counterpropagating injection pulse so that several adjacent plasma wave buckets could be filled with ultrashort electron bunches. Other variations on the colliding pulse injection concept can be readily envisioned.

In summary, the colliding laser pulse injection scheme investigated in this paper has the ability to produce relativistic femtosecond electron bunches with low fractional energy spread ($\sim 1\%$) and low normalized transverse emittance (~ 1 mm mrad). The colliding pulse scheme requires relatively low laser power compared to the pump pulse $a_1^2 \sim a_2^2 \ll a_0^2$, and allows for detailed control of the injection process through the injection phase (position of the forward injection laser pulse), the injection time (injection pulse lengths), the beat wave velocity (frequencies of the injection laser pulses), and the beat wave amplitude parameter (injection laser pulse intensities). We believe these capabilities are critical for the experimental realization of laser-triggered injection and subsequently compact laser-plasma-based particle accelerators.

ACKNOWLEDGMENTS

We acknowledge useful conversations with P. Volfbeyn and M. Zolotorev. The research at UCB was supported by the U.S. Department of Energy, Division of High Energy and Nuclear Physics Grant No. DEFG-03095ER-40936. The work at LBNL was supported by the U.S. Department of Energy under Contract No. DE-AC-03-76SF0098.

APPENDIX A: TRAPPING VOLUME

In this appendix, we calculate the region where trapping is possible (i.e., the plasma volume where the injection laser pulse amplitudes are greater than the threshold for moving an electron from an untrapped to a trapped orbit).

Consider $(\hat{a}_1\hat{a}_2)^{1/2} > (\hat{a}_1\hat{a}_2)_{\rm th}^{1/2}$, where $(\hat{a}_1\hat{a}_2)_{\rm th}^{1/2}$ is defined by Eq. (9), such that the beat wave separatrix overlaps well both the untrapped plasma fluid orbit and the plasma wake separatrix. From Eq. (1), the momentum of trapped and untrapped electrons in the plasma wake satisfies the relations

$$H+\phi=[1+u_{\rm trap}^2]^{1/2}-\beta_\varphi u_{\rm trap}, \tag{A1}$$

$$1+\phi=[1+u_{\rm untrap}^2]^{1/2}-\beta_\varphi u_{\rm untrap}, \tag{A2}$$

where $H \leqslant \phi_o+\gamma_\varphi^{-1}$ for a trapped orbit and $H \leqslant \gamma_\varphi^{-1}$ for a trapped and focused orbit.

To determine the region in wake phase ψ where trapping is possible, consider the phase ψ_1 where the maximum beat wave momentum equals the momentum of the wake separatrix,

$$(u_{\rm beat})_{\rm max}=u_{\rm trap}(\psi_1), \tag{A3}$$

and the phase ψ_2 where the minimum beat wave momentum equals the fluid momentum,

$$(u_{\rm beat})_{\rm min}=u_{\rm untrap}(\psi_2). \tag{A4}$$

The maximum and minimum momentum of the beat wave separatrix $u_{\rm beat}$ are given by Eq. (4). Applying these conditions, Eqs. (A3) and (A4), to the plasma wake Hamiltonian relations, Eqs. (A1) and (A2), yields

$$H+\phi(\psi_1)=[1+(u_{\rm beat})_{\rm max}^2]^{1/2}-\beta_\varphi(u_{\rm beat})_{\rm max}, \tag{A5}$$

$$1+\phi(\psi_2)=[1+(u_{\rm beat})_{\rm min}^2]^{1/2}-\beta_\varphi(u_{\rm beat})_{\rm min}. \tag{A6}$$

By solving for ψ_1 and ψ_2 we obtain

$$\cos\psi_1=\phi_o^{-1}[\gamma_b\gamma_\perp(0)(1-\beta_\varphi\beta_b) - 2\gamma_b(\beta_\varphi-\beta_b)(\hat{a}_1\hat{a}_2)^{1/2}-H], \tag{A7}$$

$$\cos\psi_2=\phi_o^{-1}[2\gamma_b(\beta_\varphi-\beta_b)(\hat{a}_1\hat{a}_2)^{1/2} + \gamma_b\gamma_\perp(0)(1-\beta_\varphi\beta_b)-1]. \tag{A8}$$

Note that $|\psi_2| \leqslant |\psi_1|$ and $\psi_1=\psi_2=\psi_{\rm opt}$ when $(\hat{a}_1\hat{a}_2)^{1/2}=(\hat{a}_1\hat{a}_2)_{\rm th}^{1/2}$.

If the right-hand side (RHS) of Eq. (A8) satisfies $|{\rm RHS}|<1$, then the wake phase regions where trapping is possible are $-|\psi_1| \leqslant \psi \leqslant -|\psi_2|$ and $|\psi_2| \leqslant \psi \leqslant |\psi_1|$. If solutions to Eq. (A8) do not exist [i.e., the RHS of Eq. (A8) satisfies $|{\rm RHS}|>1$], then the minimum beat wave momentum is less than the fluid momentum for all wake phases $(u_{\rm beat})_{\rm min} < u_{\rm untrap}(0)$, and the wake phase region where trapping is possible is $-|\psi_1| \leqslant \psi \leqslant |\psi_1|$. These regions are correct for injection into a trapped orbit $H=\phi_o+\gamma_\varphi^{-1}$ [where solutions to Eq. (A8) exist for typical parameters], and for injection into a trapped and focused orbit $H=\gamma_\varphi^{-1}$ [where the RHS of Eq. (A8) satisfies $|{\rm RHS}|>1$ for typical parameters].

The above Hamiltonian theory can be used to estimate the initial trapping volume in 3D, assuming $k_p r_{s0}>1$ such that the radial motion of the electrons in the plasma wake remains small. The wake phase region where trapping is possible is a function of the radial position of the electrons via Eqs. (A7) and (A8) along with the generalizations $\hat{a}_i=\hat{a}_i(r)$ and $\phi_o=\phi_o(r)$ given by Eqs. (11), (12), and (14). Figure 12 shows the region $(\psi, r(\psi))$ where trapping of plasma electrons is possible for the parameters given in Table I. In Fig. 12, the maximum radial postition where trapping is possible $r_{\rm max}$ is $r_{\rm max}=4.2$ μm, and the length of the

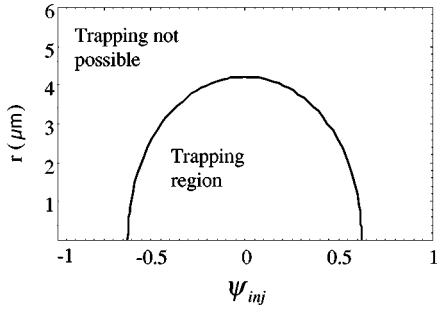

FIG. 12. Region in (ψ,r) where trapping of plasma electrons is allowed for parameters in Table I.

wake phase region where trapping is possible $L_{\rm tr}=c\omega_p^{-1}(2|\psi_1(0)|)$ is $L_{\rm tr}=7.9\ \mu$m. The volume where trapping is allowed is

$$V_{\rm tr}=\int \pi r^2(\psi)d\psi. \tag{A9}$$

For Fig. 12 the trapping volume is $V_{\rm tr}\simeq 3.0\times 10^{-10}\ {\rm cm}^{-3}$.

With the trapping region known, one can choose the injection laser pulse lengths to be greater than the wake phase region where trapping is possible, $L_i>L_{\rm tr}$, thereby maximizing the number of electrons trapped. Figure 13 shows the length of the wake phase region $L_{\rm tr}$ (solid line) and the maximum radial position $r_{\rm max}$ (dashed line) versus beat wave amplitude parameter for the parameters in Table I.

APPENDIX B: ELECTRON BUNCH DYNAMICS

In this appendix, we calculate the dynamical motion for a trapped electron bunch in a plasma wake. The longitudinal equations of motion for the electron bunch in the ultrarelativistic limit are

$$\frac{d\gamma}{d\tau}=\vec{\beta}\cdot\frac{c\partial\phi}{\omega_p\partial\vec{x}}\simeq-\phi_0\sin\psi, \tag{B1}$$

$$\frac{d\psi}{d\tau}=\beta_z-\beta_\varphi\simeq 0, \tag{B2}$$

where $\tau=\omega_p t$. The phase slippage is taken to be zero, $d\psi/dt\simeq 0$. This will be valid for interaction lengths much shorter than the dephasing length $L_{\rm dephase}\sim\lambda_p\gamma_\varphi^2$ (i.e., interaction times much shorter than the bounce time in a trapped plasma wake orbit). With these assumptions, Eqs. (B1) and (B2) have solutions

$$\gamma=\gamma_0-\phi_0\tau\sin\psi_0, \tag{B3}$$

$$\psi=\psi_0. \tag{B4}$$

With zero (or constant) phase slippage, the rms phase spread $\sigma_\psi^2=\langle\psi^2\rangle-\langle\psi\rangle^2$ is constant,

$$\frac{d\sigma_\psi}{d\tau}=\frac{1}{\sigma_\psi}\left[\left\langle\psi\frac{d\psi}{d\tau}\right\rangle-\langle\psi\rangle\left\langle\frac{d\psi}{d\tau}\right\rangle\right]=0. \tag{B5}$$

We assume a Gaussian distribution in wake phase of the trapped electrons,

$$\frac{dN}{d\psi_0}=\frac{1}{\sqrt{2\pi\sigma_\psi^2}}\exp\left[\frac{-(\psi_0-\langle\psi_0\rangle)^2}{2\sigma_\psi^2}\right], \tag{B6}$$

where the expectation value of an arbitrary function $f(\psi_0)$ is

$$\langle f(\psi_0)\rangle=\int\frac{dN}{d\psi_0}f(\psi_0)d\psi_0. \tag{B7}$$

From Eq. (B3), the mean energy of the electron bunch assuming a Gaussian distribution in wake phase Eq. (B6) is

$$\langle\gamma\rangle=\langle\gamma_0\rangle-\phi_0\tau e^{-\sigma_\psi^2/2}\sin\langle\psi_0\rangle. \tag{B8}$$

Assuming the initial conditions γ_0 and ψ_0 are uncorrelated (statistically independent) such that $\langle\gamma_0\psi_0\rangle=\langle\gamma_0\rangle\langle\psi_0\rangle$, the rms energy spread $\sigma_\gamma^2=\langle\gamma^2\rangle-\langle\gamma\rangle^2$ is

$$\sigma_\gamma^2=\sigma_{\gamma_0}^2+\frac{1}{2}\phi_0^2\tau^2(1-e^{-\sigma_\psi^2})(1+e^{-\sigma_\psi^2}\cos[2\langle\psi_0\rangle]). \tag{B9}$$

Using Eqs. (B8) and (B9), the fractional energy spread is

$$\frac{\sigma_\gamma}{\langle\gamma\rangle}=\frac{\pm\sqrt{\sigma_{\gamma_0}^2+\frac{\phi_0^2\tau^2}{2}(1-e^{-\sigma_\psi^2})(1+e^{-\sigma_\psi^2}\cos[2\langle\psi_0\rangle])}}{\langle\gamma_0\rangle-\phi_0\tau e^{-\sigma_\psi^2/2}\sin\langle\psi_0\rangle} \tag{B10}$$

with the asymptotic value (for large τ)

$$\frac{\sigma_\gamma}{\langle\gamma\rangle}\to\frac{\sqrt{\frac{1}{2}(1-e^{-\sigma_\psi^2})(1+e^{-\sigma_\psi^2}\cos[2\langle\psi_0\rangle])}}{e^{-\sigma_\psi^2/2}\sin\langle\psi_0\rangle}. \tag{B11}$$

For $\sigma_\psi\ll 1$, Eq. (B11) simplifies to

$$\frac{\sigma_\gamma}{\langle\gamma\rangle}\simeq\sigma_\psi\cot\langle\psi_0\rangle. \tag{B12}$$

The asymptotic form of the fractional energy spread Eq. (B11) has a minimum value at a phase of $\langle\psi_0\rangle=\pi/2$ (at the crest of the plasma wake), $[\sigma_\gamma/\langle\gamma\rangle]_{\rm min}\to\sqrt{2}\sinh(\sigma_\psi^2/2)\simeq\sigma_\psi^2/\sqrt{2}$. As Eq. (B11) indicates, the asymptotic fractional

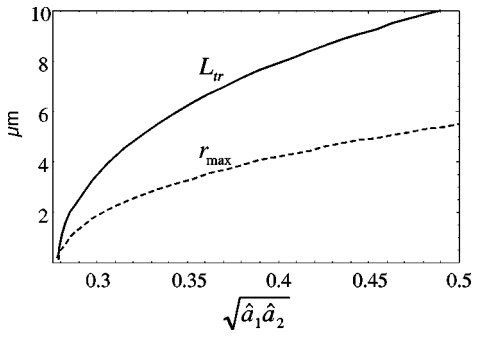

FIG. 13. The length of the wake phase region $L_{\rm tr}$ (solid line) and the maximum radial position $r_{\rm max}$ (dashed line) where trapping is possible versus beat wave amplitude parameter $(\hat{a}_1\hat{a}_2)^{1/2}$.

energy spread is independent of the wake amplitude, and is just a function of the phase and the rms phase spread, which is constant assuming zero (or constant) phase slippage. For illustration, consider the numerical simulation shown in Fig. 8. Once the bunch becomes highly relativistic, $\langle\psi\rangle\simeq -13.9$ and $\sigma_\psi\simeq 0.17$. With these values, the asymptotic fractional energy spread predicted by Eq. (B12) is $[\sigma_\gamma/\langle\gamma\rangle]\simeq 0.04$, in good agreement with the numerical simulation Fig. 8(c).

The normalized longitudinal rms emittance of the trapped electron bunch is $\varepsilon_\parallel^2=\sigma_\gamma^2\sigma_\psi^2-\sigma_{\gamma\psi}^2$, where $\sigma_{\gamma\psi}=\langle\gamma\psi\rangle-\langle\gamma\rangle\langle\psi\rangle$. With the assumptions $\sigma_\psi\ll 1$ and a Gaussian distribution in phase Eq. (B6), the normalized longitudinal rms emittance is

$$\varepsilon_\parallel^2=\sigma_{\gamma_0}^2\sigma_\psi^2+\frac{1}{2}\phi_0^2\tau^2\sigma_\psi^6\sin\langle\psi_0\rangle. \tag{B13}$$

The longitudinal rms emittance of the trapped electron bunch $\varepsilon_\parallel$ grows linearly for large τ. This emittance growth is due to the fact that the bunch becomes relativistic at a wake phase where the energy gain is nonlinear with respect to the wake phase.

[1] T. Tajima and J. Dawson, Phys. Rev. Lett. **43**, 267 (1979).

[2] J. S. Wurtele, Phys. Fluids B **5**, 2363 (1993).

[3] E. Esarey, P. Sprangle, J. Krall, and A. Ting, IEEE Trans. Plasma Sci. **PS-24**, 252 (1996).

[4] P. Kung, H. Lihn, H. Wiedemann, and D. Bocek, Phys. Rev. Lett. **73**, 967 (1994); B. E. Carlsten and S. J. Russel, Phys. Rev. E **53**, 2072 (1996); X. J. Wang, X. Qui, and I. Ben-Zvi, *ibid.* **54**, 3121 (1996).

[5] E. Esarey, R. F. Hubbard, W. P. Leemans, A. Ting, and P. Sprangle, Phys. Rev. Lett. **79**, 2682 (1997).

[6] D. Umstadter, J. K. Kim, and E. Dodd, Phys. Rev. Lett. **76**, 2073 (1996).

[7] R. G. Hemker, K.-C. Tzeng, W. B. Mori, C. E. Clayton, and T. Katsouleas, Phys. Rev. E **57**, 5920 (1998).

[8] E. Esarey, B. Hafizi, R. Hubbard, and A. Ting, Phys. Rev. Lett. **80**, 5552 (1998).

[9] A. Modena, Z. Najmudin, A. E. Dangor, C. E. Clayton, K. A. Marsh, C. Joshi, V. Malka, C. B. Darrow, C. Danson, D. Neely, and F. N. Walsh, Nature (London) **377**, 606 (1995).

[10] K. Nakajima, D. Fisher, T. Kawakubo, H. Nakanishi, A. Ogata, Y. Kato, Y. Kitagawa, R. Kodama, K. Mima, H. Shiraga, K. Suzuki, K. Yamakawa, T. Zhang, Y. Sakawa, T. Shoji, Y. Nishida, N. Yugami, M. Downer, and T. Tajima, Phys. Rev. Lett. **74**, 4428 (1995); C. Coverdale, C. B. Darrow, C. D. Decker, W. B. Mori, K. C. Tzeng, K. A. Marsh, C. E. Clayton, and C. Joshi, *ibid.* **74**, 4659 (1995).

[11] D. Umstadter, S. Y. Chen, A. Maksimchuk, G. Mourou, and R. Wagner, Science **273**, 472 (1996); R. Wagner, S. Y. Chen, A. Maksimchuk, and D. Umstadter, Phys. Rev. Lett. **78**, 3125 (1997).

[12] A. Ting, C. I. Moore, K. Krushelnick, C. Manka, E. Esarey, P. Sprangle, R. Hubbard, H. R. Burris, and M. Baine, Phys. Plasmas **4**, 1889 (1997); C. I. Moore, A. Ting, K. Krushelnick, E. Esarey, H. F. Hubbard, B. Hafizi, H. R. Burris, C. Manka, and P. Sprangle, Phys. Rev. Lett. **79**, 3909 (1997).

[13] D. Gordon, K. C. Tzeng, C. E. Clayton, A. E. Dangor, V. Malka, K. A. Marsh, A. Modena, W. B. Mori, P. Muggli, A. Najmudin, D. Neely, C. Danson, and C. Joshi, Phys. Rev. Lett. **80**, 2133 (1998).

[14] E. Esarey and M. Pilloff, Phys. Plasmas **2**, 1432 (1995).

[15] A. Yariv, *Quantum Electronics* (Wiley, New York, 1989).

[16] E. Esarey, A. Ting, P. Sprangle, and G. Joyce, Comments Plasma Phys. Control. Fusion **12**, 191 (1989).

[17] W. H. Press, B. P. Flannery, S. A. Teukolsky, and W. R. Vetterling, *Numerical Recipes: The Art of Scientific Computing* (Cambridge Univ. Press, Cambridge, 1986).

[18] E. P. Lee and R. K. Cooper, Part. Accel. **7**, 83 (1976).

[19] T. Katsouleas, S. Wilks, P. Chen, J. M. Dawson, and J. J. Su, Part. Accel. **22**, 81 (1987).